Article

4R-Cembranoid Treatment Alters Gene Expression of RAW264.7 Macrophages in Basal and Inflammatory Conditions

Maxine N. Gonzalez-Vega[1,2], Sandeep Sreerama[2], Kelvin Carrasquillo-Carrion[3], Abiel Roche [3], Susan Corey Best[5], Kiminobu Sugaya[2], Pedro A. Ferchmin[4], Vesna A. Eterovic[4], Antonio H. Martins[5*]

1. Universidad Central del Caribe, Neuroscience Department; Ave. Laurel #100, Santa Juanita, Bayamón, P.R., 00956. Tel: (787) 798-3001

2. University of Central Florida, Burnett School of Medicine; 6900 Lake Nona Blvd, Orlando, FL 32827. Tel: (407) 266-7045

3. University of Puerto Rico, Medical Sciences Campus, Biomedical Data Science Department; Guillermo Arbona Irizarry Bld, San Juan, P.R. 00936-5067. Tel: (787) 758-2525 Ext. 2194

4. Universidad Central del Caribe, Biochemistry Department; Ave. Laurel #100, Santa Juanita, Bayamón, P.R., 00956. Tel: (787) 798-3001

5. University of Puerto Rico, Medical Sciences Campus, Pharmacology and Toxicology Department; Calle Los Paseos, Guillermo Arbona Bldg, San Juan, PR 00935. Tel: (787) 758-2525 Ext. 1300 or 1304.

*Author to whom correspondence should be addressed:

Dr. Antonio H. Martins; Tel.787-758-2525, Fax: 787-766-4441; antonio.martins@upr.edu

Abstract: Inflammation is considered an important target for stroke therapy because it induces secondary brain damage after the initial ischemic insult. Peripheral monocytes migrate to the brain parenchyma after a central insult. They then differentiate to macrophages in a positive feedback fashion contributing to damage instead of ischemic resolution and inflammation control. A cyclic diterpenoid, (1S,2E,4R,6R,7E,11E)-cembra-2,7,11-triene-4,6-diol (4R), decreases neurodegeneration after ischemia with central anti-inflammatory activity. This study aims to determine whether the central anti-inflammatory effect of 4R is effective against peripheral inflammation triggered by brain ischemia. To investigate the anti-inflammatory effect of 4R, we treated macrophages with lipopolysaccharide (LPS) as an inflammatory model, followed by treatment with 4R. Microarray transcriptome analysis of over 30,000 genes identified the differential expression of 393 genes. Genes related to inflammation, cell adhesion, and

transcription were validated with qPCR, and reduced expression was determined. Quantification of NF-kB phosphorylation served as a marker for the modulation of inflammation through gene transcription. Our results show that 4R was associated with a reduction in NFKB1 and ITGB5 gene expression, increased phosphorylation of NF-kB, and a decrease in macrophage adhesion in a blood-brain barrier model. These results indicate that 4R can partially modulate the peripheral immune response, making 4R a potential drug against post-ischemic inflammation.

Keywords: cembranoid; inflammation; macrophage, NF-kB, adhesion

---

1. Introduction

Stroke is medically defined as a disease that affects arteries conducting to or in the brain, affecting the proper supply of blood. It is the second leading cause of death and adult disability worldwide [1]. Neuronal death initiates glutamate excitotoxicity that causes a toxic effect on the surrounding tissue, propagating an inflammatory signaling cascade responsible for increasing the ischemic damage caused by stroke [2–5]. A few days after the initiation of ischemia, brain inflammation causes the recruitment of peripheral monocytes, which are responsible for regulating the transition from acute inflammation to chronic inflammation [6]. The inflammatory factors produced by macrophages influence the activation, migration, and effector function of partner inflammatory cells by changing the inflammatory response, either in the resolution of inflammation or the propagation of tissue damage [7]. Macrophages are essential producers of cytokines, chemokines, and adhesion molecules, as well as other inflammatory factors that are critical signaling mechanisms for host defense from pathogenic infection to traumatic injuries [8].

Unfortunately, effective drugs that target chronic inflammation in the central nervous system (CNS) have not yet been discovered. Therefore, there is an urgent need to identify new safe molecules that can modulate central inflammation after an ischemic insult. Peripheral immunity depends on a set of signaling and adhesion

molecules such as integrins and cell adhesion molecules (CAMs) that permit the infiltration of macrophages into the affected tissue.

A cyclic diterpenoid, (1S,2E,4R,6R,7E,11E)-cembra-2,7,11-triene-4,6-diol, termed 4R, has been found to provide CNS protection in neurodegenerative diseases [9,10] and exposure to an analog of sarin, the neurotoxic gas [11]. Moreover, 4R has been shown to decrease expression of intercellular adhesion molecule 1 (iCAM-1) and vascular cell adhesion molecule 1 (vCAM-1) in a murine brain-derived endothelial cell line, bEND5, that serves as a blood-brain barrier model under normal and pathologic conditions such as stroke, Parkinson's disease, and inflammation [9,10]. The direct central neuroprotection and decreased reactivity of astrocytes, which can be considered a decrease of inflammation [12], provided by 4R is triggered by processes that involve the Akt pathway [11]; however, little is known about the modulatory mechanisms of peripheral inflammation.

Olsson (1993) reported that 4R inhibits prostaglandin synthesis in seminal bovine microbiomes with an IC_{50} of 390μM [13], supporting the notion that 4R possesses the capacity of modulating inflammation. These changes in the inflammatory microenvironment will influence the activation of astrocytes, as well as the recruitment of the peripheral immune system. In this study, we examine the peripheral inflammatory modulatory capacity of 4R and its role in the adhesion of macrophages to human brain microvascular cells, a model of the blood-brain barrier, thus expanding and reproducing its effect in bEND5 endothelial cells [9].

2. Materials and Methods

2.1 Cell Cultures and Maintenance Reagents

2.1.1 RAW264.7 Cells

The murine macrophage cell line RAW264.7 was obtained from the American Type Cell Culture (ATCC, Virginia, USA, cat. #TIB-71) and cultured in complete DMEM (cDMEM) [10% FBS, 100 units/mL of Penicillin and 100µg/mL streptomycin), 1% non-essential amino acids (100x, Thermo Fisher formulation) and 2mM L-glutamine] and maintained at 37°C with 5% CO_2. The medium was changed every 2-3 days, and cells were passed using a cell scraper before they reached 95% confluence. For experiments, 2×10^6 RAW264.7 cells were plated in 60 mm tissue culture-treated dishes and left overnight to recover. Macrophages were treated with 5µM of 4R (stock 20mM), 0.025% polyethylene glycol/ ethanol at a ratio of 90%/10% v/v, respectively (PEG/Eth), and/or 100ng/mL LPS (stock 0.1mg/mL).

2.1.2 hCMEC/D3 cells

Immortalized human cerebral microvascular endothelial cells (hCMEC/D3) were purchased from Millipore Sigma (Darmstadt, Germany, cat. #SCC066). Cells were cultured to confluence in EBM-2 basal medium (Lonza) supplemented with a proprietary formulation MV-Bullet Kit from Lonza [for 500mL final volume, FBS (12.5mL), R3-IGF-1 (125µL), VEGF (125µL), human EGF (125µL), hydrocortisone (50µL), human bFGF (5µL)], and 100 units/mL of penicillin and 100µg/mL streptomycin. Cultured cells were maintained at 37°C with 5% CO_2, changing the media every 2-3 days, and sub-cultivating every five days. For experiments, 2×10^5 hCMEC/D3 cells were seeded in a 24-well tissue culture treated-plate and maintained for 24hrs to allow monolayer formation.

2.2 Comprehensive transcriptome analysis

The murine macrophage cell line, RAW264.7, was plated at 2×10^6 cells per dish (60 mm tissue culture-treated dishes). Once flasks reached 90% confluence, the cells were treated with 100ng/mL LPS in fresh cDMEM for 2hrs (see flowchart, **Fig. 1**). Then the cells were washed with cDMEM twice and treated with 5μM 4R or vehicle (0.025% PEG/Eth) for 1hr. The treatment was followed by two washes with cDMEM, and cells were left to rest for 2hrs in fresh cDMEM, allowing time to respond to the given stimuli. After treatment, cells were collected using the cell-scrapper and pelleted by centrifugation at 500 x g for 10minutes. The cell pellet was stored at -80°C. Samples were processed for comprehensive transcriptome analysis at the University of Puerto Rico Medical Sciences Campus (San Juan, PR, Core Facility) using the GeneChip WT Pico Kit (902622; Affymetrix) and the GeneChip Mouse Transcriptome Pico Assay 1.0 (902663; Affymetrix).

2.3 Ingenuity Pathway Analysis (IPA)

For the analytical section, data processing and differential expression analysis were performed using the Bioconductor software packages oligo and limma. The microarray raw intensity values were processed in the Affymetrix CEL file format using the Robust Multi-array Average (RMA) algorithm from the oligo package. Background correction was done, log2 transformed and normalized by quantile normalization. The statistical analysis was conducted using the limma software package. Case versus control group analysis was performed with the following data sets, with three replicates per group: 4R vs. PEG/Eth, and [4R with LPS] vs. [PEG/Eth with LPS]. Differentially expressed genes were defined as having a Fold-Change (FC) ≥2 and p-value ≤ 0.05). The differentially expressed genes for both comparisons were

submitted for Ingenuity Pathway Analysis of Apoptosis-, Proliferation-, and Inflammation-related pathways and networks.
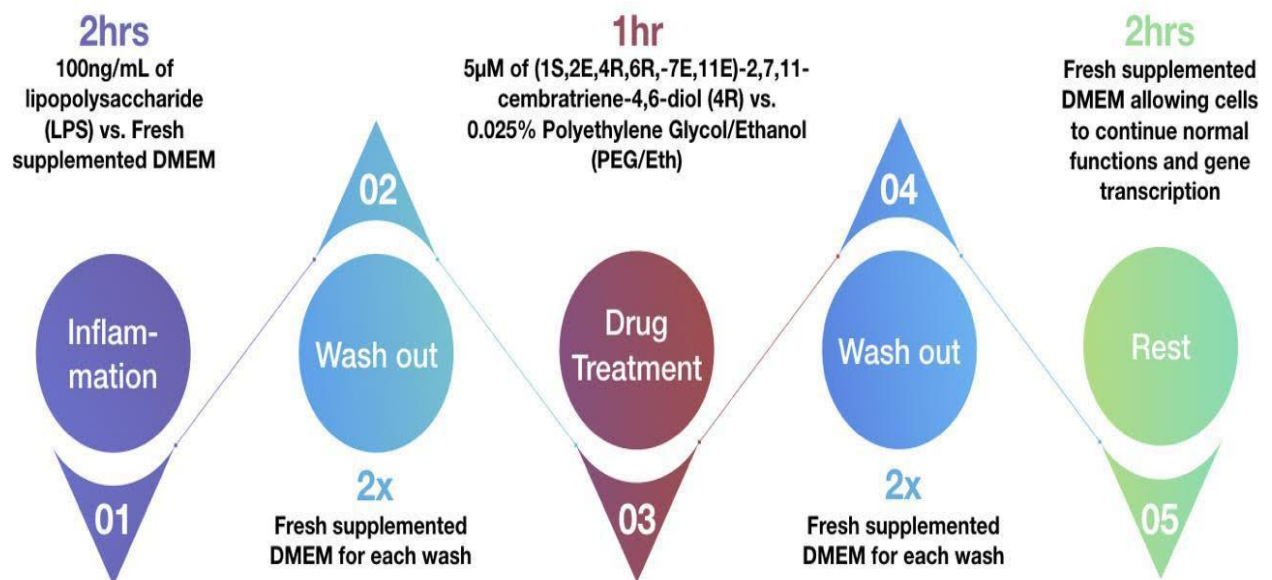

Figure 1. Timeline for treatment of RAW264.7 cells with 4R and/or LPS for transcriptome analysis.

2.4 Real-time quantitative PCR

Total RNA was isolated from samples treated according to the LPS ± 4R microarray timeline (**Fig. 1**) and the 6hrs simultaneous treatments in RAW264.7 macrophage cells. Macrophages were treated for 6hrs continuously with the drug compound or vehicle in the presence and absence of LPS. RNA was isolated using the Direct-zol RNA MiniPrep (Zymo Research), treated in the column with DNAse I, and RNA quality was determined with a NanoDrop™ 8000 Spectrophotometer (Thermo Scientific). In total, 1.0μg of RNA were reverse-transcribed into cDNA using a SuperScript III First-Strand Synthesis SuperMix qRT-PCR (Invitrogen). Real-time quantitative PCR was performed in a 7500 Fast Real-Time PCR System (Life Technologies) for IL-1β, NFKBIE, NFKB1, CCL5, ITGB5, iCAM, MCP-1, iNOS, and β-Actin targets. Primers (**Table 1**) were purchased from Eurofins Genomics.

Quantitative PCR was performed in duplicates in a total volume of 20μL containing 100ng of RNA reverse-transcribed to cDNA, 10μL of SYBR Green PCR Master Mix (Applied Biosystems), and 300nM primer concentration. Cycling conditions for the quantitative RT-PCRs were as follows: 95°C for 10 min, followed by 40 cycles at 95°C for 15 seconds and 60°C for 60 seconds. Analysis of the melting curves demonstrated that each pair of primers amplified a single product. Relative changes in mRNA expression for the genes were assessed by the $2^{-\Delta\Delta Ct}$ method using the corresponding mRNA expression for vehicle-treated samples (PEG/Eth, and LPS+PEG/Eth) as a calibrator (set to a value of 1). Samples were classified into two groups of basal and LPS stimulation, and then an unpaired t-test was performed for the samples for each gene and group using Prism7.

Table 1. Primers used for qRT-PCR analysis.

Gene	Forward (5' → 3')	Reverse (5' → 3')	Accession Num.	Reference or Primer Bank ID	Product Size
IL1Beta	GCAACTGTTCCTGAACTCAACT	ATCTTTTGGGGTCCGTCAACT	NM_008361.4	Tomita et al., 2016	89
MCP1	TGATCCCAATGAGTAGGCTGGAG	ATGTCTGGACCCATTCCTTCTTG	NM_011333.3	Diamond et al., 2007	132
iNOS	TTCACCCAGTTGTGCATCGACCTA	TCCATGGTCACCTCCAACACAAGA	NM_001313922.1	Tomita et al., 2016	140
iCAM1	CAATTTCTCATGCCGCACAG	AGCTGGAAGATCGAAAGTCC	NM_010493.3	Ren et al., 2010	103
NFKBIE	TGGACCTCCAACTGAAGAACT	TTCCTCTGCAATGTGGCAATG	NM_008690.4	31543321a1	64
NFKB1	ATGGCAGACGATGATCCCTAC	TGTTGACAGTGGTATTTCTGGTG	NM_008689.2	30047197a1	111
ITGB5	GAAGTGCCACCTCGTGTGAA	GGACCGTGGATTGCCAAAGT	NM_001145884	225007620c1	86
CCL5	GCTGCTTTGCCTACCTCTCC	TCGAGTGACAAACACGACTGC	NM_013653.3	7305461a1	104
GAPDH	CTCCCACTCTTCCACCTTCG	GCCTCTCTTGCTCAGTGTCC	NM_001289726.1	Ruiz-Villalba et al., 2017	189

2.5 Immunoblotting

RAW264.7 cells previously treated with LPS ± 4R for 1hr (see **Fig. 1**) were washed twice with PBS and collected by scraping with a cell scraper, while immersed in 1mL of PBS to avoid cell-damage. The cells were pelleted by centrifugation at 300 x g for 10 minutes, then resuspended in ice-cold M-Per lysis buffer (Thermo Scientific) supplemented with protease and phosphatase inhibitor cocktail (2mM 4-Benzenesulfonyl fluoride hydrochloride, 0.3µM Aprotinin, 130µM Bestatin, 1mM EDTA, 14µM E-64 and 1µM leupeptin) (Sigma-Aldrich) and allowed to rest for 20 mins. With 2 minutes intervals, samples were vortexed for 10sec. The cell-debris pellet was collected by centrifuging the cells at 16.3×10^3 x g at 4ºC for 10 minutes; the supernatant was collected, and the insoluble pellet was discarded. Total protein was measured using the BCA assay (Pierce Thermo Scientific). From the cell lysates, 15µg of total protein in NuPAGE LDS buffer and reducing agent was heated at 70°C for 10 minutes and cooled on ice for 5 minutes. The proteins were separated on 10% NuPAGE SDS-polyacrylamide gel (Invitrogen) together with PageRuler Plus prestained protein ladder (Thermo Scientific) and transferred to a nitrocellulose membrane 0.45µm (Schleicher & Schuell; Grade BA85). After blocking with 5% nonfat milk in Tris-buffered saline, 0.1% Tween-20 (TBST) for 1hr at room temperature (23°C), the membranes were incubated with specific antibodies overnight at 4°C. The following primary antibodies were purchased from Cell Signaling Technology: p65 total (1:1000, #6956; stock concentration 50.0µg/mL), p65 phosphorylation Ser536 (1:1000, #3033; stock concentration 57.0µg/mL), and β-Actin (1:5000, #4970; stock concentration 116.0µg/mL). HRP-conjugated secondary antibodies (Cell Signaling Technology) were used at a 1:5000 dilution (stock concentration 0.8mg/mL). The antigen-antibody complexes were visualized using the enhanced chemiluminescence West Femto Detection System (Thermo Fisher) according to the manufacturer's protocol. ImageJ software was used to detect the intensity value reading for each sample within the sample blot. Using Prism7

samples were classified and divided into groups of basal drug treatment and LPS-stimulated macrophages, then an unpaired t-test performed detected any changes in protein intensity.

2.6 Adhesion Assay

The hCMECD3 human cerebral microvascular endothelial cells were incubated for 24hrs with 100ng/mL LPS incubation. After 24hrs, 4R (5μM) or PEG/Eth (0.025%) was added for the remaining 24hrs period. The 4R-treated cells were stained with Vybrant DiO (10μL/mL) (Molecular Probes, cat. #V22886) for 30 minutes (see Timeline, **Fig. 2**). The hCMECD3 monolayer cells were washed three times with PBS, and 1×10^6 DiI$^+$ stained RAW264.7 macrophages (pre-stained with 0.3mg/mL DiI$^+$ for 1hr, Molecular Probes, cat. #D282) were added to the monolayer and maintained for 1hr at 37°C with 5% CO_2. Cells were washed three times with PBS to remove any non-adherent macrophages and fixed with 1mL of 4% paraformaldehyde/PBS with subsequent incubation for 20 minutes at 4°C. Using 1x Phosphate Buffer Saline (PBS, pH 7.4), cells were washed twice and counterstained for cell nuclei using DAPI (4',6-diamidino-2-phenylindole) at a concentration of 1μg/mL for 10 minutes. Microscopy data were collected from a minimum of four fields of view per sample (12 fields of view in total for each treatment), done in biological triplicate. Images were taken using Zeiss 710 with the Zeiss AxioObserver microscope (lens: LD Plan Neofluar 20x/0,4 Ph2 Korr 421351-9970) and analyzed using ImageJ cell count.
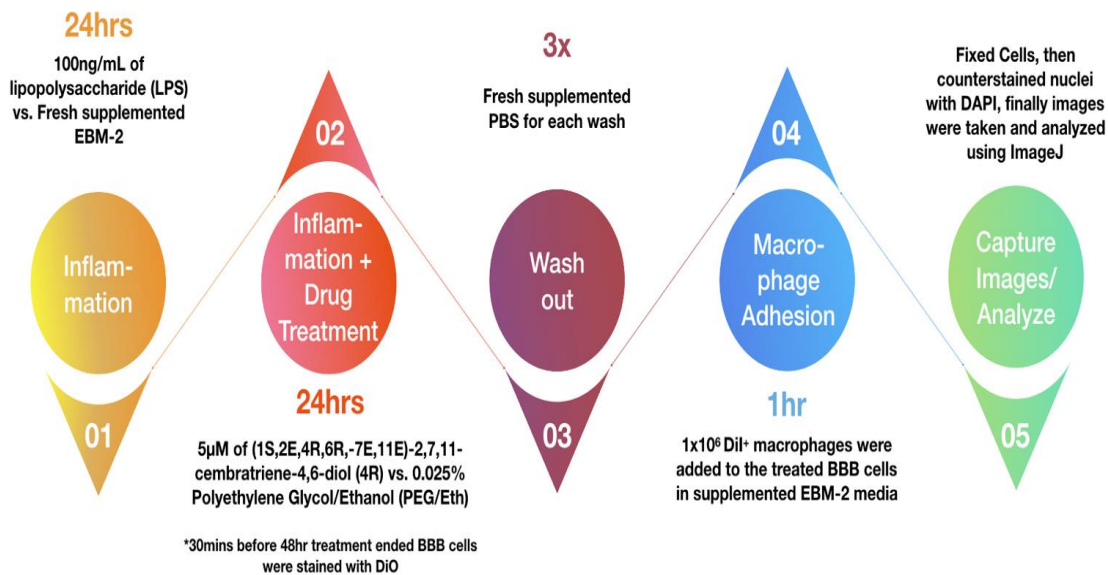
Figure 2. Timeline of LPS ± 4R treatment for adhesion assay.

3. Results

3.1 4R treatment alters gene expression in murine macrophages responsible for canonical pathways involved in inflammation and cell survival.

Treatment with 4R after inflammatory treatment with LPS regulates an array of genes involved in mediating select cell responses, including inflammation, viral protection, and proliferation when compared to the vehicle groups, PEG/Eth, or LPS + PEG/Eth. A total of 393 genes (302 up-regulated and 91 down-regulated) were identified and color-coded in a volcano plot (**Fig. 3A-B**). Genes that were not regulated by 4R treatment are shown in black, and these are considered natural variation within cell samples and not due to the treatments.

Of the 302 genes that were upregulated, 33% are associated with inflammation, implying activation of the pathways involved. Of the 91 down-regulated genes, 86%

are involved in cell cycle function. Canonical pathways regulated by 4R (**Fig. 3C**) include DNA replication (22 genes), NF-kB (18 genes), Toll-like Receptor Signaling (13 genes), IL-6 Signaling (13 genes), Interferon (12 genes), TNF-α (12 genes), Apoptosis (10 genes), ERK/MAPK (7 genes), Cytokine-Cytokine Receptor Interaction (7 genes), G2/M DNA Damage Checkpoint Regulator (5 genes) and Cytokine Signaling (4 genes). Genes involved in inflammation and cell cycle were selected to compare expression under normal and inflammatory conditions after 4R treatment (**Fig. 3D**). For most of the selected genes, 4R treatment under basal conditions appeared to decrease the expression of inflammatory genes (IL1A, RSAD2, and CCL5), and up-regulate genes involved in macrophage differentiation and cell migration (CXCR4 and S1PR1, respectively). Specific fold changes for selected genes are shown in **Table 2**. Notably, post-inflammatory 4R-treatment up-regulated genes involved in inflammatory responses in peripheral macrophages after LPS. However, this did not translate into the propagation of cell damage in previously published *in vivo* experiments [9–11,14,15]. The post-inflammatory response to 4R could mean that 4R modulates inflammation in a manner that provides additional immediate support, but not prolonged enough to produce damage. Also, it strongly suggests that the inflammatory mechanism of action is through a signaling pathway that includes NF-kB.

3.2 qPCR validation of select microarray genes, determined a modulation of iNOS, NFKB1, ITGB5, and IL-1Beta in murine macrophage cells treated with 4R on basal and LPS conditions

Under basal conditions (**Fig. 1**), 4R did not significantly alter expression of IL-1Beta, NFKBIE, NFKB1, iNOS, CCL5, ITGB5, ICAM1, and MCP1 (FC= 1.34±0.19, 1.17±0.1, 1.08±0.17, 1.77±0.16, 0.82±0.09, 1.1±0.12, 1.02±0.04, and 0.96±0.12, respectively, mean±SEM). Similar mRNA expression patterns were observed for most genes for the 4R group when compared to the vehicle group (**Figs. 3A** and **4A**). Only iNOS expression was up-regulated 2-fold by 4R treatment for 1hr (**Fig. 5A**). Induction of mRNA for all genes was evident after LPS stimulation for 2hrs before drug treatment when compared to basal conditions (**Table S1-S2**). Post-4R treatment to LPS stimulated macrophages decreased the mRNA of NFKB1 and ITGB5 (FC= 0.72±0.029, and 0.77±0.01, respectively, mean±SEM) (**Fig. 4B**). There was no difference between 4R and PEG/Eth controls in the expression patterns of IL-1Beta, NFKBIE, iNOS, CCL5, ICAM1, and MCP1 mRNA after LPS treatment (**Fig. 4B**): (FC= 0.98±0.07, 1.17±0.10, 0.71±0.13, 0.87±0.06, 0.81±0.09, and 1.22±0.14, mean±SEM respectively).
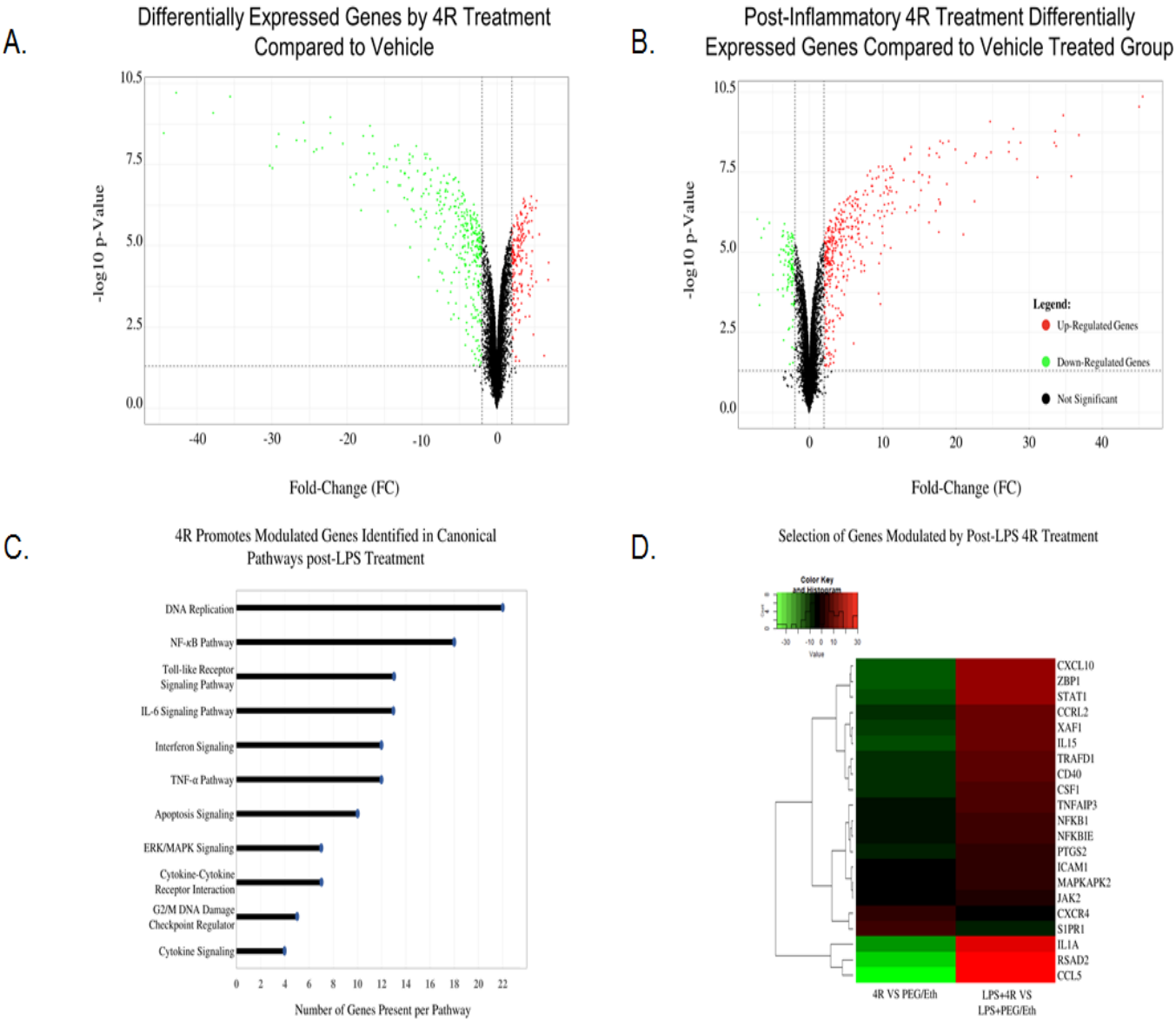
Figure 3. 4R treatment modulates under basal and inflammatory conditions the expression of key genes in RAW264.7 macrophages. A, B. Volcano maps of gene expression fold changes. Plots of fold changes versus significance (-log P value) in macrophages. Down-regulated genes are represented by green dots, up-regulated genes by red dots, and un-regulated genes by black dots. The horizontal line represents p< 0.05, and the two vertical lines represent ± 2-fold change. **A.** Fold changes in macrophages treated with 4R versus vehicle-only. **B.** Fold changes in macrophages treated with LPS ± 4R. **C.** Classification of selected genes modulated by 4R that are involved in canonical pathways of inflammation and cell viability. Most of the genes are associated with DNA replication or the NF-κB pathway. **D.** A heat map of selected fold changes in two conditions, 4R vs control in basal conditions and 4R vs vehicle after LPS. Green represents down-regulation (-FC), red represents the up-regulation of gene expression, and black represents no significant change.

Table 3.2. Genes in the Heatmap plot. Genes found in the heatmap plot with the fold change for each cluster (4R vs PEG/Eth and LPS+4R vs LPS+PEG/Eth). Genes selected were based on those found in the canonical pathways studied. *gene not found in the heatmap.

Gene Name	Gene Fold-Change (p<=0.05)	
	4R vs PEG/Eth	LPS+4R vs LPS+PEG/Eth
CCL2	-11.32	15.27
CCRL2	-9.59	11.89
CCL5	-37.77	33.67
CD40	-9.43	8.54
CSF1	-8.025	7.09
CXCL10	-14.54	17.87
CXCR4	2.50	-3.67
ICAM1	-2.36	3.17
IL1A	-22.16	27.89
IL1B	-30.23	33.50
IL15	-11.91	11.67
*ITGB5**	3.00	-2.95
JAK2	-2.11	2.14
MAPKAPK2	-2.27	2.31
NFKB1	-4.45	5.17
NFKBIE	-3.88	4.31
NOS2	-4.43	4.25
PTGS2	-5.77	3.99
RSAD2	-29.91	33.75
S1PR1	4.28	-6.15
STAT1	-12.82	16.43
TNFAIP3	-4.67	6.96
TRAFD1	-9.57	10.02
XAF1	-11.20	5.36
ZBP1	-14.63	16.32
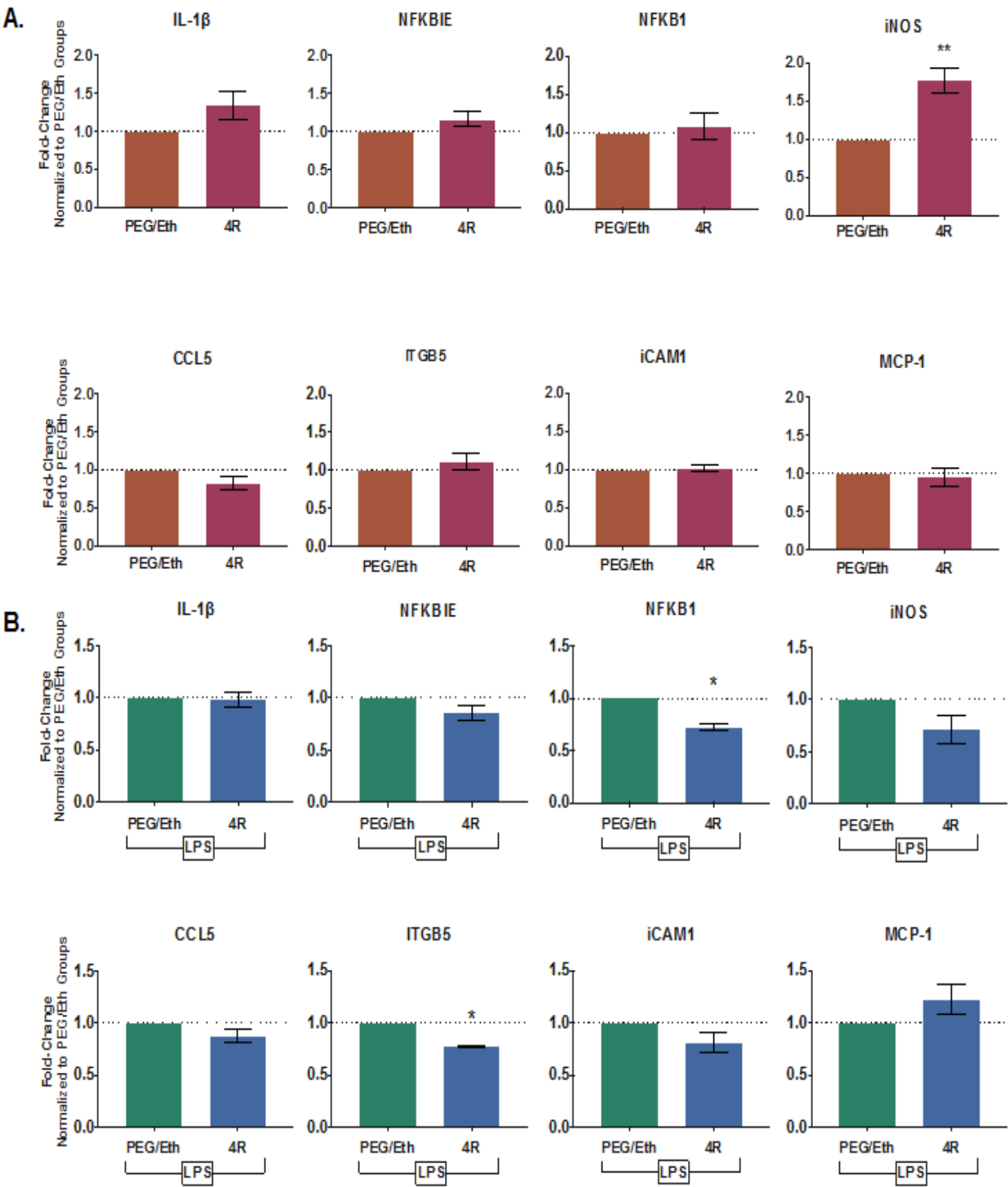
Figure 4. Validation by quantitative PCR of genes identified in Fig. 3 sequential treatment of RAW264.7 macrophages with LPS and 4R (Fig. 1) . A. Gene validation for qRT-PCR with vehicle and 4R treatment for IL-1B, NFKBIE, NFKB1, iNOS, CCL5, ITGB5, iCAM1, and MCP-1. 4R treatment increased iNOS gene expression when compared to PEG/Eth, whereas all other tested genes showed no modulation for basal conditions. **B.** The same genes validated with the LPS inflammatory insult for both PEG/Eth and 4R: Treatment with 4R decreased gene expression of NFKB1 and ITGB5. Plot of the mean ± SEM, statistical analysis used, Unpaired T-Test, *p < 0.05, **(P=0.001 to 0.01); n=3
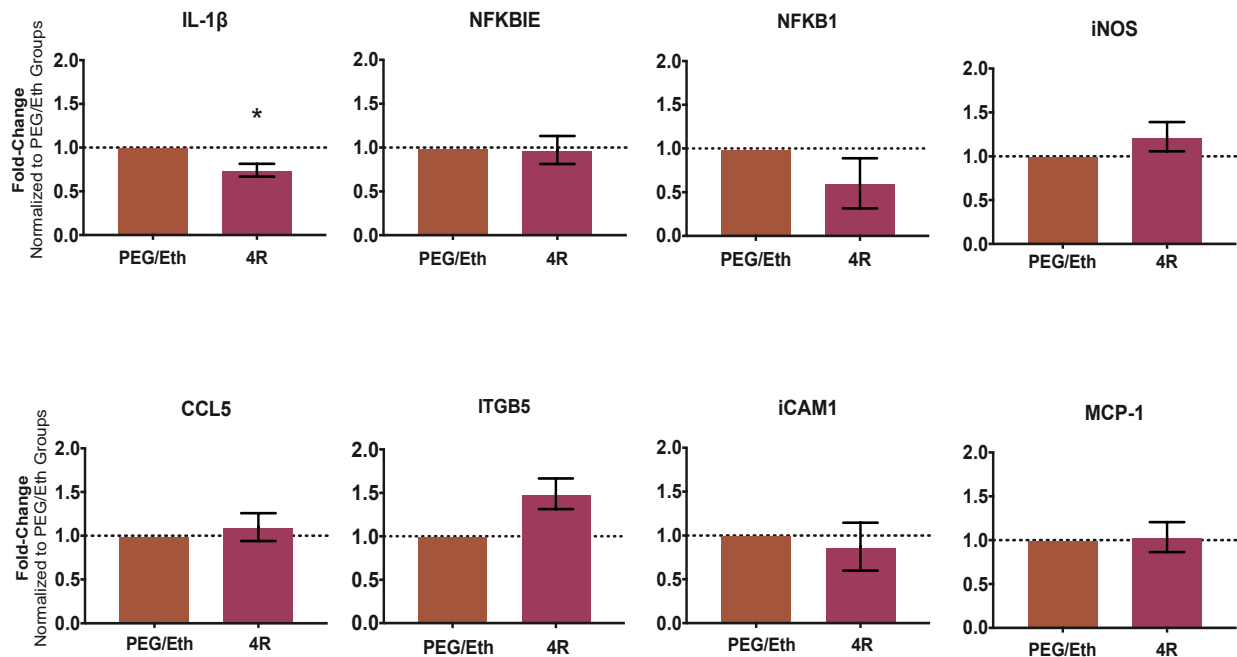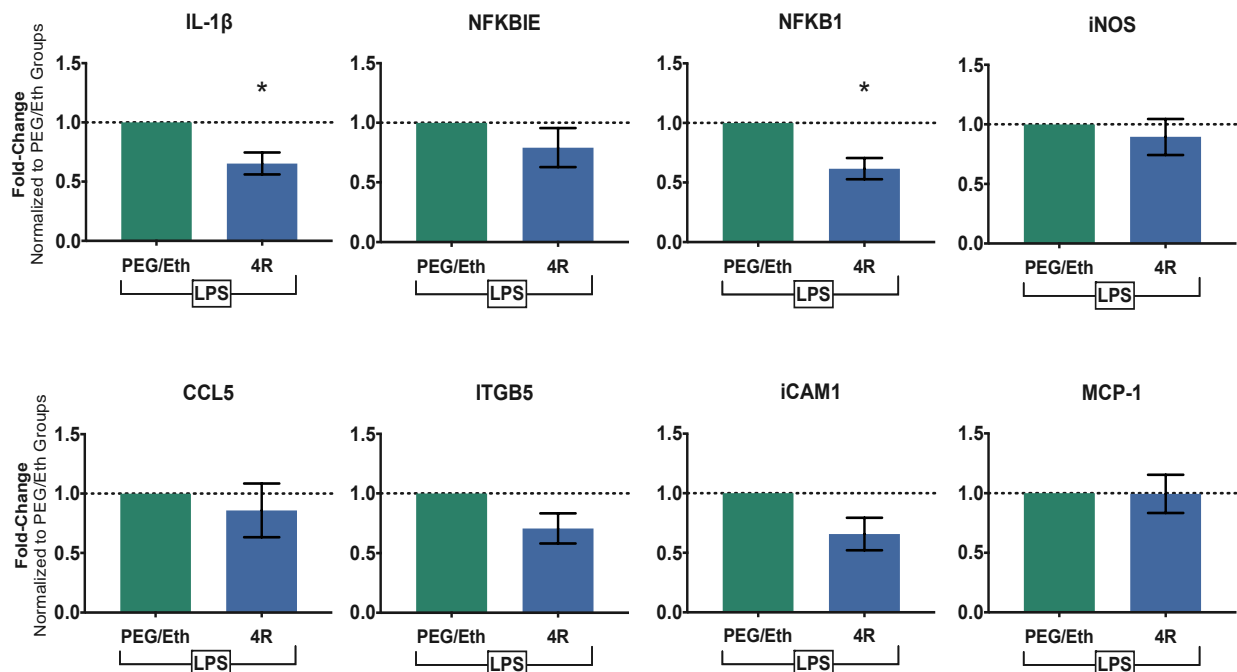
Figure 5. Quantitative PCR of inflammatory genes following 6hrs incubation of macrophages with LPS ± 4R. A. Genes tested for validation (IL-1B, NFKBIE, NFKB1, iNOS, CCL5, ITGB5, iCAM1, and MCP-1) were quantified for simultaneous treatment of 4R or vehicle. Basal 6hrs treatment of 4R decreased IL-1B genes when compared to PEG/Eth. All other tested genes showed similar patterns between 4R and drug vehicle groups. **B.** The simultaneous 6hrs treatment with LPS and 4R showed down-regulation of IL-1B and NFKB1 genes. The data presented are mean ± SEM. Unpaired T-Test, *p < 0.05; n=3

In contrast, 6hrs stimulation of macrophages with 4R alone decreased mRNA of IL-1Beta (FC= 0.74±0.073, mean±SEM) when compared to the PEG/Eth group; the remaining genes showed no differences in mRNA expression (**Fig. 5A**). Simultaneous incubation with 4R or vehicle and LPS for 6hrs produced decreases in IL-1Beta and NFKB1 gene expression (FC= 0.65±0.09, 0.62±0.089, respectively, mean±SEM); no significant differences were found in the expression of mRNA for NFKBIE, iNOS, CCL5, ITGB5, ICAM1, and MCP1 for both LPS+4R and LPS+PEG/Eth groups (FC= 0.97±0.16, 0.92±0.15, 0.86±0.23, 0.71±0.13, 0.66±0.14, and 0.99±0.16, respectively, mean±SEM) (**Fig. 5B**). A consistent downregulation of NFKB1 mRNA expression was seen in both the microarray timeline protocol (**Fig. 1**) and the 6hrs simultaneous incubation of macrophages with 4R or vehicle in the presence of LPS.

3.3 Simultaneous treatment with 4R and LPS promotes an early increase in the activation of NF-kB through the Ser536 phosphorylation of p65

Detecting phosphorylation of p65 at the TAD site indicates that p65 has moved to the nucleus and has begun gene transcription. The expression of phosphorylated Ser536 p65 was not significantly different from vehicle PEG/Eth under basal conditions (p65 Ser536 116.1±15.82%, compared to the mean value for PEG/Eth normalized to 100). Stimulation with LPS for 1hr increased overall protein expression, and co-incubation with 4R enhanced the increase (120.7±7.77%, mean±SEM vs. control) (**Fig. 6A**). Total p65 protein was significantly increased under basal conditions with 4R treatment for 6hrs (p65 total 4R mean±SEM, 113.9±5.003%) when compared to the vehicle-treated group. In contrast, total p65 was unchanged when incubated with LPS ± 4R or vehicle for 6hrs (total p65 =106.3±7.911% vs. normalized control, mean±SEM) (**Fig. 6B**). The normalized values

for the p65 Ser536 and p65 total for each treatment were divided to determine the ratio of activation for each treatment. Under basal conditions, 4R treatment did not modulate the ratio of p65 phosphorylation (p65 ser536/total p65 after 4R, 104.7±20.72%, mean±SEM), but the ratio of phosphorylated ser536 to p65 did increase following LPS stimulation with 4R treatment for 6hrs (mean±SEM of ratios of normalized values, 126.9±11.07%) (**Fig. 6C**).

The 4R compound has been shown to modulate $\alpha 4\beta 2$ and $\alpha 7$ nicotinic receptors activity [16]; these receptors are known to have a downstream activation effect on p50/p65 activation. Additionally, LPS activates toll-like receptor 4, ultimately activating the NF-kB pathway. Therefore, the simultaneous activation of these pathways may explain the increased expression of the p65 Ser536 phosphorylation in macrophages co-treated with 4R and LPS (**Fig. 6D**). Activation of this pathway is known to lead to an inflammatory response of macrophages.

3.4 4R decreases the adhesion of peripheral murine macrophages to the hCMEC/D3 cells, a model of the blood-brain barrier (BBB) after 48hrs of LPS stimulation.

Macrophage cells are key modulators of inflammation in the host. However, when it comes to CNS inflammation, they have to adhere, and then infiltrate the BBB to mediate any injury. Excess peripheral infiltration of macrophages to the CNS will prolong and disseminate damage in the brain. In the presence of an insult, the BBB increases in adherent proteins that act as anchors for peripheral immune cells, and this phenomenon also occurs in macrophages via integrins and cell adhesion molecules [17].

Validated 4R promoted downregulation of ITGB5 for microarray samples, indicates a modulation in macrophage tissue invasion at a genetic phase. To test the functional effect of 4R on macrophage adhesion, DiI⁺ stained macrophages were exposed to

hCMEC/D3 cells treated for 48hrs with LPS or left in basal conditions. After the first 24hrs of inflammation insult, 4R or PEG/Eth was added for the remaining 24hrs (**Fig. 7A**). Macrophages that remained adhered to hCMEC/D3 after intensive washes were counted, and the overall ratio was determined as adhesion. Basal conditions showed no change in adhesion of DiI$^+$ stained macrophages when comparing 4R and PEG/Eth groups (macrophages per DAPI, 0.12±0.015, and 0.17±0.02, respectively, mean±SEM) (**Fig. 7B**). As expected, incubation with LPS and PEG/Eth increased the adhesion of DiI$^+$ macrophages to hCMEC/D3 cells (0.36±0.04 macrophages/DAPI mean±SEM). The co-incubation of 4R with LPS significantly decreased the adhesion of macrophages compared with incubation of LPS with PEG/Eth (adhesion/DAPI, 0.23±0.03, mean±SEM) (**Fig. 7C**), to a level similar to control conditions (control adhesion, 0.21±0.02, mean±SEM).

4. Discussion

These studies demonstrate that 4R, a neuroprotective compound that easily crosses the BBB and accumulates in the brain, can be used as a lead compound for future anti-inflammatory therapy after an ischemic stroke. We have shown that 4R decreases macrophage adhesion to a cell model of the blood-brain barrier following inflammatory stimulation. 4R also downregulates NF-kB. Currently, there are no therapeutic measures that target the post-ischemic inflammatory response. However, several agents are under clinical studies, and some already licensed to treat other inflammatory diseases are being evaluated for their capability to reduce inflammation after brain ischemia.

After brain ischemia, the live neurons in the penumbra tissue suffer from deleterious signals, deteriorate, and die. The damaged or dead neurons release a series of inflammatory and death factors such as caspases and molecules, which change the microenvironment to initiate a local immune response from microglia

and astrocytic cells. Local immunity will target the inflammatory insult via the production of more signaling molecules, phagocytosis, and the activation/recruitment of peripheral immunity [18–21]. Local inflammation induces a breakdown in the blood-brain barrier to permit peripheral leukocytes to migrate into the brain parenchyma. Primary macrophage and neutrophil infiltration commence a series of responses that contribute to a preliminary protective effect in the brain. However, studies have shown that prolonged activation of macrophages proves to be detrimental to the brain by the engulfment of healthy neurons [22,23].

4R is a natural cembranoid derived from the tobacco leaves and flower. It does not have a noxious effect when used in rats up to 98mg/kg [16]. Olsson and colleagues (1993) tested the anti-inflammatory effect of 4R on the activity of cyclooxygenase type two (COX2) in seminal bovine vesicle microsomes [13]. A decrease in COX2 activity was produced by 4R at a concentration of 397μM, considerably higher than the EC_{50} at 0.8μM at which 4R induces neuroprotection in *ex vivo* hippocampal slices [24,25]. In the present work, treatment with LPS and 4R at 1.53μg/mL (5μM) differentially regulated close to 400 genes related to canonical pathways from the cell cycle to inflammation. Microarray analysis determined that among the inflammatory canonical pathways, genes associated with the NF-kB signaling pathway were positively modulated by 4R treatment.

The NF-kB family is comprised of 5 subunits (RelA/p65, cRel, RelB, p50, p52), forming dimers that are generally inactive before post-translational modifications (PTM). The PTMs lead to conformational changes and detachment of inhibitor of kappa B proteins (IκBα, IkBβ, IkBε, Bcl3, and IkBζ), permitting nuclear translocation and transcriptional activity [26]. The NF-kB cascade transcribes genes for diverse cell functions ranging from apoptosis, proliferation, survival, adhesion, invasion, and inflammatory responses [27]. Among the dimers formed, the most abundant and

directly related to inflammation is the p65/p50 subunit found in different cell types and hosts [26,28]. In this study, 4R treatment showed gene modulation that correlates with those transcribed by the p65/p50 dimer, the predominant dimer that mediates inflammation [29], and genes directly involved in the NF-kB pathway, such as the upregulation of the NFKB1 gene.
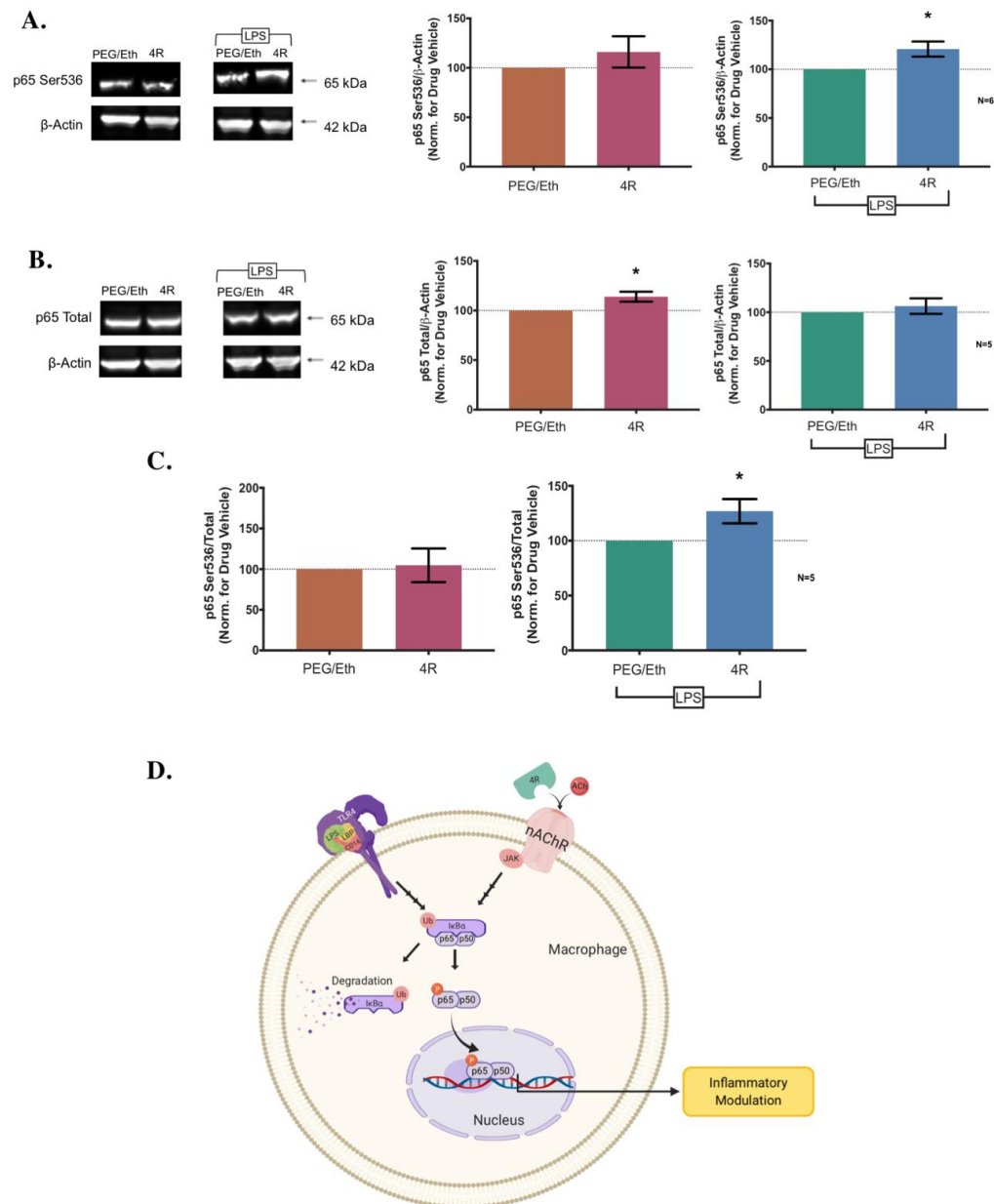
Figure 6. 1hr Treatment with 4R increased p65 phosphorylation at the serine 536 site, indicating an increase in NF-kB activation in macrophages. A. Expression of phosphorylated ser536 p65 under basal conditions and following co-incubation with LPS + 4R or vehicle (PEG/Eth) for 1hr. (n=6). **B.** Total p65 protein expression in macrophages treated with 4R or vehicle under basal or inflammatory conditions. **C.** The ratio of p65 ser536 to total p65 was increased by co-incubation with LPS and 4R, suggesting increased proportion of activated form ready for nuclear translocation. **D.** Diagram of a suggested mechanism of action for 4R and LPS in macrophages resulting in cell response. Created with BioRender.com, figure exported under a paid subscription. Data represent the mean ± SEM of 5-6 independent experiments.
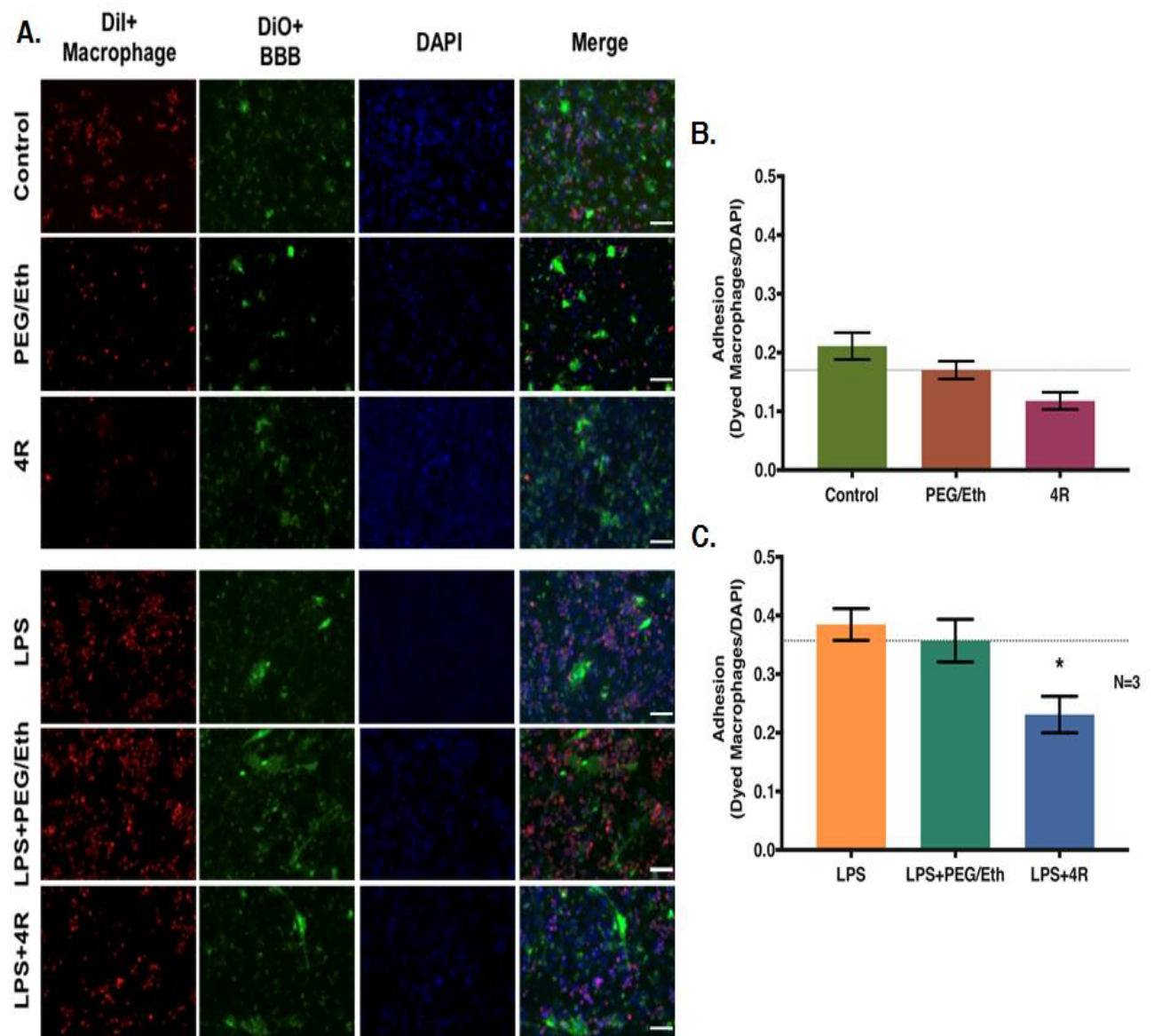
Figure 7. Post-inflammatory treatment of 4R decreases overall macrophage adhesion to the BBB after an inflammatory stimulus to the barrier. A. hCMEC/D3 cells were stained with DiO cells (green cells); macrophages were stained with DiI (red). All cell nuclei were labelled with DAPI, then images were merged to differentiate between free and macrophage-bound hCMEC/D3 cells. **B.** Under control conditions, adhesion of macrophages is detected, but 4R treatment does not reduce DiI+ macrophage adhesion. **C.** In LPS simulation groups, DiI+ macrophage adhesion increases when compared to control conditions. 4R treatment after inflammation induction with LPS reduces adhesion of macrophages to the BBB to a basal level (similar to PEG/Eth) when compared to both LPS and LPS+PEG/Eth group. One-Way ANOVA, Kruskal-Wallis test, with Dunn's multiple comparison test, *p < 0.05.

The p50 homodimer does not possess the transcriptional capacity by itself due to the lack of the transactivation domain (TAD) in the p50 subunits, the domain that helps the dimer bind and transcribe the target DNA. Hence, studying the activation of the p65 subunit of the p50/p65 dimer correlates with the potential inflammatory role of 4R. There are a series of PTMs for the p65 subunit that leads to its activation and translocation to the nucleus; the most frequently studied is the phosphorylation of Ser536 in the TAD sequence. This phosphorylation serves as an indicator that the complex will translocate to the nucleus, leading to inflammatory gene transcription.

Under basal conditions, 4R treatment does not modulate the phosphorylation of the Ser536 of p65 in the times, and concentrations studied. The increase in phosphorylation on this site by LPS indicates the activation of p65. Although a one-hour treatment with dexamethasone (1μM), is not enough to modulate LPS-stimulate activation of p65 (data not shown), 4R treatment increases this activation when compared to the samples treated with the drug vehicle, PEG/Eth. The activation of the p65 protein occurs rapidly; however, the latent effect leads to the transcription of cytokines and chemokines that continue to modulate the inflammatory response of the macrophages.

Post-inflammatory 4R treatment upregulates genes involved in inflammatory responses of macrophages. However, this did not translate in damage propagation when using *in vivo* experiments previously published [9], suggesting that 4R modulates inflammation in a manner that provides additional immediate support, but not prolonged enough, validated by the adhesion of macrophages to the BBB. Inhibition of the NF-kB signaling cascade, inhibits the adhesion and chemoattraction of monocytes/macrophages [12], determining that any modulation of the NF-kB pathway will affect the infiltration of peripheral macrophages. However, the confirmed 4R treatment increase of p65 activated form, translates to a reduced

adhesive capacity of macrophages to the BBB after an inflammatory insult, suggesting that 4R minimizes the invasion of macrophages to the CNS. Reducing the immune cells readily activated and providing a wave of inflammatory molecules could help the CNS restore homeostasis by not prolonging the inflammatory response in ischemic stroke. Direct neuroprotection by 4R in stroke provides an immediate benefit for the host [9], and now there is evidence that suggests that this protection can also include a decrease of inflammation.

Supplementary Materials: The following are available online at www.mdpi.com/xxx/s1, Figure S1: title, Table S1: title, Video S1: title.

Samples	GAPDH	IL-1Beta	NFKBIE	ITGB5	NFKB1	CCL5	iCAM1	MCP1	INOS
	C_T (Mean ± SEM)
PEG/Eth	12.54±0.3384	29.29±0.4844	22.78±0.3378	23.3±0.8646	21.64±0.7482	26.89±1.57	22.87±1.215	22.79±1.223	31.41±0.547
4R	12.92±0.435	29.24±0.5143	22.96±0.2215	23.77±1.009	22.29±0.9952	27.58±1.853	23.23±1.378	23.26±1.267	30.98±0.4795
LPS+PEG/Eth	12.72±0.3662	15.65±0.07586	21.14±0.3131	25.34±1.002	19.54±0.8916	16.61±1.191	20.79±1.101	16.97±0.9341	21.54±0.71
LPS+4R	12.83±0.3995	15.8±0.2754	21.46±0.2718	25.81±0.9355	20.12±0.7977	16.92±1.428	21.22±1.397	16.8±0.9531	22.19±0.3698

Table S1. C_T values (mean±SEM) of microarray treated samples for gene validation. GAPDH C_T values are constant between all samples. For genes IL1B, NFKBIE, NFKB1, CCL5, ICAM1, MCP1 and INOS it shows a lower C_T value for samples treated with LPS when compared to basal conditions. However, for ITGB5, LPS treatment decreases the C_T values when compared to drug treated basal conditions.

Samples	GAPDH	IL-1Beta	NFKBIE	ITGB5	NFKB1	CCL5	iCAM1	MCP-1	iNOS
	C_T (Mean ± SEM)
PEG/Eth	14.68±0.4803	30.52±0.3371	24.1±1.121	26.29±2.039	25.55±3.009	27.88±0.8746	25.32±1.406	23.51±0.8612	31.99±1.264
4R	15.06±0.7734	31.35±0.7224	24.57±1.339	26.86±2.011	26.98±3.919	28.16±1.202	26.03±1.81	23.88±1.293	32.11±1.377
LPS+PEG/Eth	14.62±0.2553	17.83±1.023	22.99±0.4001	26.31±0.1201	21.85±2.123	16.88±0.2867	22.16±0.5895	16.46±0.7704	20.42±0.6021
LPS+4R	13.9±0.4231	17.75±1.39	22.68±0.06882	26.14±0.4742	21.86±2.386	16.49±0.05655	22.11±0.3039	15.78±0.697	19.9±0.5459

Table S2. C$_T$ values (mean±SEM) of 6hrs continued drug with or without LPS treatment to compares gene expression to microarray timeline. GAPDH C$_T$ values are within a range for all samples. The C$_T$ values for the ITGB5 gene is not altered by LPS treatment when compared to basal conditions drug treated. For IL1B, NKFBIE, NFKB1, CCL5, ICAM1, MCP1, and INOS, basal conditions show a higher C$_T$ value, and LPS treatment lowers the C$_T$ value needed to surpass the threshold established.

Conceptualization, Maxine N. Gonzalez-Vega, Vesna A. Eterovic, Pedro A. Ferchmin, and Antonio Henrique Martins; Formal analysis, Maxine N. Gonzalez-Vega; Funding acquisition, Pedro A. Ferchmin, and Antonio Henrique Martins; Methodology, Maxine N. Gonzalez-Vega, Sandeep Sreerama, and Antonio Henrique Martins; Project administration, Kiminobu Sugaya, Pedro A. Ferchmin, and Antonio Henrique Martins; Resources, Kiminobu Sugaya, and Antonio Henrique Martins; Supervision, Antonio Henrique Martins; Validation, Maxine N. Gonzalez-Vega, Kelvin Carrasquillo-Carrion, and Abiel Roche-Lima; Visualization, Maxine N. Gonzalez-Vega; Writing – original draft, Maxine N. Gonzalez-Vega; Writing – review & editing, Susan Corey Best, Kiminobu Sugaya, Vesna A. Eterovic, Pedro A. Ferchmin, and Antonio Henrique Martins.

Conflicts of Interest: The authors declare no conflict of interest.

References

1. Young, M.J.; Regenhardt, R.W.; Leslie-Mazwi, T.M.; Stein, M.A. Disabling stroke in persons already with a disability: Ethical dimensions and directives. *Neurology* **2020**.

2. Lai, T.W.; Zhang, S.; Wang, Y.T. Excitotoxicity, and stroke: identifying novel targets for neuroprotection. *Prog Neurobiol* **2014**, *115,* 157–188.

3. Chamorro, A.; Dirnagl, U.; Urra, X.; Planas, A.M. Neuroprotection in acute

stroke: targeting excitotoxicity, oxidative and nitrosative stress, and inflammation. *Lancet Neurol* **2016**, *15*, 869–881.

4. Castillo, J.; Davalos, A.; Noya, M. Progression of ischaemic stroke and excitotoxic aminoacids. *Lancet* **1997**, *349*, 79–83.

5. Hazell, A.S. Excitotoxic mechanisms in stroke: an update of concepts and treatment strategies. *Neurochem Int* **2007**, *50*, 941–953.

6. Atri, C.; Guerfali, F.Z.; Laouini, D. Role of Human Macrophage Polarization in Inflammation during Infectious Diseases. *Int J Mol Sci* **2018**, *19*.

7. Cronkite, D.A.; Strutt, T.M. The Regulation of Inflammation by Innate and Adaptive Lymphocytes. *J Immunol Res* **2018**, *2018*, 1467538.

8. Cao, S.; Zhang, X.; Edwards, J.P.; Mosser, D.M. NF-kappaB1 (p50) homodimers differentially regulate pro- and anti-inflammatory cytokines in macrophages. *J Biol Chem* **2006**, *281*, 26041–26050.

9. Martins, A.H.; Hu, J.; Xu, Z.; Mu, C.; Alvarez, P.; Ford, B.D.; El Sayed, K.; Eterovic, V.A.; Ferchmin, P.A.; Hao, J. Neuroprotective activity of (1S,2E,4R,6R,-7E,11E)-2,7,11-cembratriene-4,6-diol (4R) in vitro and in vivo in rodent models of brain ischemia. *Neuroscience* **2015**, *291*, 250–9.

10. Hu, J.; Ferchmin, P.A.; Hemmerle, A.M.; Seroogy, K.B.; Eterovic, V.A.; Hao, J. 4R-Cembranoid Improves Outcomes after 6-Hydroxydopamine Challenge in Both In vitro and In vivo Models of Parkinson's Disease. *Front Neurosci* **2017**, *11*, 272.

11. Ferchmin, P.A.; Hao, J.; Perez, D.; Penzo, M.; Maldonado, H.M.; Gonzalez, M.T.; Rodriguez, A.D.; de Vellis, J. Tobacco cembranoids protect the function of acute hippocampal slices against NMDA by a mechanism mediated by alpha4beta2 nicotinic receptors. *J Neurosci Res* **2005**, *82*, 631–641.

12. Li, K.; Li, J.; Zheng, J.; Qin, S. Reactive Astrocytes in Neurodegenerative Diseases. *Aging Dis* **2019**, *10*, 664–675.

13. Olsson, E.; Holth, A.; Kumlin, E.; Bohlin, L.; Wahlberg, I. Structure-related inhibiting activity of some tobacco cembranoids on the prostaglandin synthesis in vitro. *Planta Med* **1993**, *59*, 293–295.

14. Ferchmin, P.A.; Andino, M.; Reyes Salaman, R.; Alves, J.; Velez-Roman, J.; Cuadrado, B.; Carrasco, M.; Torres-Rivera, W.; Segarra, A.; Martins, A.H.; et al. 4R-cembranoid protects against diisopropylfluorophosphate-mediated

neurodegeneration. *Neurotoxicology* **2014**, *44*, 80–90.

15. Ferchmin, P.A.; Perez, D.; Cuadrado, B.L.; Carrasco, M.; Martins, A.H.; Eterovic, V.A. Neuroprotection Against Diisopropylfluorophosphate in Acute Hippocampal Slices. *Neurochem Res* **2015**, *40*, 2143–2151.

16. Velez-Carrasco, W.; Green, C.E.; Catz, P.; Furimsky, A.; O'Loughlin, K.; Eterovic, V.A.; Ferchmin, P.A. Pharmacokinetics and Metabolism of 4R-Cembranoid. *PLoS One* **2015**, *10*, e0121540.

17. Pachter, J.S.; De Vries, H.E.; Fabry, Z. The blood-brain barrier and its role in immune privilege in the central nervous system. *J. Neuropathol. Exp. Neurol.* 2003.

18. Chamorro, A.; Meisel, A.; Planas, A.M.; Urra, X.; van de Beek, D.; Veltkamp, R. The immunology of acute stroke. *Nat Rev Neurol* **2012**, *8*, 401–410.

19. Kamel, H.; Iadecola, C. Brain-immune interactions and ischemic stroke: clinical implications. *Arch Neurol* **2012**, *69*, 576–581.

20. del Zoppo, G.J.; Becker, K.J.; Hallenbeck, J.M. Inflammation after stroke: is it harmful? *Arch Neurol* **2001**, *58*, 669–672.

21. Yenari, M.A.; Kauppinen, T.M.; Swanson, R.A. Microglial activation in stroke: therapeutic targets. *Neurotherapeutics* **2010**, *7*, 378–391.

22. Neher, J.J.; Emmrich, J. V; Fricker, M.; Mander, P.K.; Thery, C.; Brown, G.C. Phagocytosis executes delayed neuronal death after focal brain ischemia. *Proc Natl Acad Sci U S A* **2013**, *110*, E4098-107.

23. Neher, J.J.; Neniskyte, U.; Brown, G.C. Primary phagocytosis of neurons by inflamed microglia: potential roles in neurodegeneration. *Front Pharmacol* **2012**, *3*, 27.

24. Eterovic, V.A.; Perez, D.; Martins, A.H.; Cuadrado, B.L.; Carrasco, M.; Ferchmin, P.A. A cembranoid protects acute hippocampal slices against paraoxon neurotoxicity. *Toxicol Vitr.* **2011**, *25*, 1468–1474.

25. Yan, N.; Du, Y.; Liu, X.; Zhang, H.; Liu, Y.; Zhang, Z. A Review on Bioactivities of Tobacco Cembranoid Diterpenes. *Biomolecules* **2019**, *9*.

26. Cookson, V.J.; Chapman, N.R. NF-kappaB function in the human myometrium during pregnancy and parturition. *Histol Histopathol* **2010**, *25*, 945–956.

27.   Liu, T.; Zhang, L.; Joo, D.; Sun, S.C. NF-kappaB signaling in inflammation. *Signal Transduct Target Ther* **2017**, *2*.

28.   Oeckinghaus, A.; Ghosh, S. The NF-kappaB family of transcription factors and its regulation. *Cold Spring Harb Perspect Biol* **2009**, *1*, a000034.

29.   Lin, L.; DeMartino, G.N.; Greene, W.C. Cotranslational dimerization of the Rel homology domain of NF-kappaB1 generates p50-p105 heterodimers and is required for effective p50 production. *EMBO J* **2000**, *19*, 4712–4722.